

Research on Fluorinated Graphene as Cathode Active Material for Enhancing the Electrochemical Performance of Potassium Primary Batteries

Yanyan Li
School of Automotive
Engineering
Zibo Vocational Institute
Zibo 255049, PR China

Abstract: In this work, the desired reduced graphene oxide was obtained by thermal reduction and hydrothermal reduction, and it was fluorinated to obtain the fluorinated graphene (FG-0.95) required for the experiment, and then the electrochemical performance of fluorinated carbon as cathode active material of potassium primary battery was studied. Comparing the discharge curves of the fluorinated graphene and commercial fluorinated graphite (Daikin), it can be concluded that the discharge voltage platform of the FG-0.95 sample is more stable than the discharge platform of the Daikin sample, and its specific capacity is much larger than that of the Daikin sample, so that the electrochemical performance of FG-0.95 is better. The FG-0.95 sample is more suitable as a positive electrode material for a potassium fluorinated carbon primary battery.

Keywords: potassium primary battery; fluorinated graphene; fluorinated graphite; discharge; voltage

1. INTRODUCTION

Since the 1950s, research on the construction and performance of lithium fluorinated carbon batteries (LPBs) has been conducted in foreign countries. Within approximately 20 years, these low-cost, long-lasting, high-energy-density batteries have been widely applied in various fields. Currently, research hotspots in LPBs focus on improving the low-temperature performance and rate capability of the battery system by altering certain characteristics of the cathode and anode materials and seeking appropriate electrolytes. In contrast, potassium fluorinated carbon primary batteries (KPBs) have only garnered attention from scientists in recent years[1]. Lithium resources are scarce in the Earth's crust and mostly concentrated in South America, leading to a severe shortage of lithium resources in many countries. This situation has significantly hindered technological progress. Therefore, it is crucial to find abundant resources to replace lithium-based energy storage systems. Lithium and potassium belong to the same group (Group 1) in the periodic table, sharing similar chemical and physical properties[2]. However, potassium resources are more abundant than lithium resources, attracting the attention of many scientists.

Analogous to LPBs, we can explore KPBs. KPBs use metallic potassium as the anode material and powdered fluorinated carbon as the cathode material, constituting a primary battery. Fluorinated carbon, as the cathode material, is considered one of the most valuable materials in primary battery research[3]. Many primary batteries have achieved significant breakthroughs by using fluorinated carbon as the cathode material. Fluorinated carbon materials are widely used in various primary batteries, exhibiting good performance in high-temperature, high-pressure, and corrosive environments. Due to its low density and interwoven layered microstructure, carbon fluoride can be added to gasoline[4]. The development and application of various other fluorinated carbon materials have injected new vitality into the construction and research of many primary batteries. Fluorinated carbon plays a crucial role in the construction of primary batteries because it is a

very stable substance that does not decompose at certain high temperatures. However, as a cathode material in batteries, fluorinated carbon has a drawback: during battery operation, the electrical conductivity decreases as the fluorine content increases, leading to a significant voltage lag during the initial discharge stage[5]. Consequently, fluorinated carbon cannot fully meet the requirements for normal battery operation when used as a cathode material, and its application is therefore limited. Therefore, finding a new and efficient method to modify carbon fluoride materials is crucial for the development of potassium-carbon fluoride primary batteries.

In this work, we prepared the fluorinated graphene with the F/C ratio of 0.95. Comparing the discharge curves of the fluorinated graphene and commercial fluorinated graphite (Daikin), it can be concluded that the discharge platform of the FG-0.95 sample is more stable than the discharge platform of the Daikin sample, and its specific capacity is much larger than that of the Daikin sample, so that the electrochemical performance of FG-0.95 is better.

2. EXPERIMENTAL

Graphene was prepared by modified Hummers method. The desired reduced graphene oxide was obtained by hydrothermal reduction at 150°C and then thermal reduction at 800°C. Further, it was fluorinated at 450°C to obtain the fluorinated graphene (FG-0.95). Microscopic morphology of materials was observed by the scanning electron microscope (SEM) and transmission electron microscope (TEM). X-ray diffraction (XRD) was used to characterize the crystal structure of the samples. Then, CR2032 coin cells were assembled in an argon-filled glovebox using the prepared potassium foils as the cathode electrodes, and 1 M KPF₆ in EC:DMC:EMC (1:1:1) as the electrolyte.

3 RESULTS AND DISCUSSION

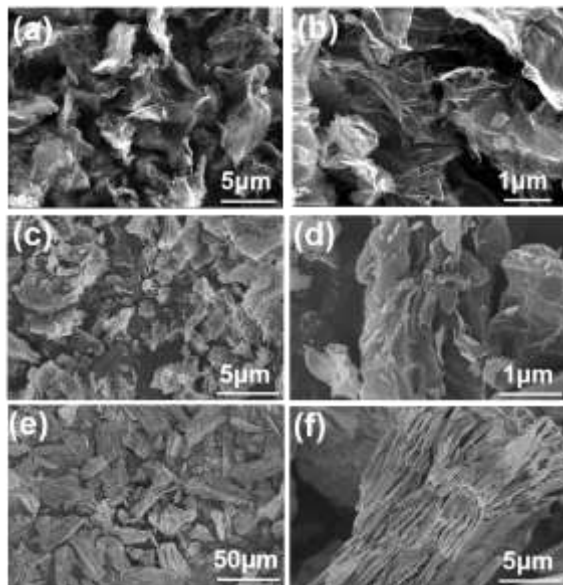


Fig.1 SEM images of materials.

Fig. 1 displays the electron micrographs of samples under different scanning electron microscope (SEM) resolutions. Fig.1a-b shows the SEM image of unfluorinated reduced graphene oxide (RGO). It can be observed that the unfluorinated RGO exhibits a lamellar structure. Fig.1c-d presents the SEM image of fluorinated graphene with a F/C ratio of 0.95 (FG-0.95). From this image, it is evident that the previously lamellar graphene structure has been divided into transformed into small particles. This is because the fluorination reaction involves the incorporation of fluorine atoms into the carbon layers, converting C-C bonds into C-F bonds. When a significant number of fluorine atoms penetrate the surface of the carbon layers, the carbon layers are disrupted, manifesting as the division of graphene sheets into small particles. Fig. 1e-f depicts the SEM image of the Daikin sample, revealing a bulk structure. It can be found that its thickness is greater than that of graphene, indicating that this sample is composed of multiple layers of graphene stacked together. Based on the above analysis and comparison, it can be concluded that the Daikin sample exhibits a bulk form overall, while the FG-0.95 sample presents a lamellar structure with the emergence of some small granular fluorinated graphene particles.

Fig.2 presents the transmission electron microscope (TEM) images and X-ray diffraction (XRD) patterns of the samples. Fig.1a shows the TEM image of unfluorinated reduced graphene oxide, revealing a clear interlayer spacing of approximately 0.33 nm. Fig1. b and c depict the FG-0.95 sample and the Daikin sample, respectively. It can be observed from these images that the layered structure disappears after fluorination. Further insights into this structure can be gained through the XRD pattern, as shown in Fig.1d. The peak at $2\theta = 26.28^\circ$ (002) belongs to the structure of unfluorinated reduced graphene oxide. Using the Scherrer equation, $D = k\lambda / (\beta \cos\theta)$, the interlayer spacing of unfluorinated reduced graphene oxide is calculated to be 0.33 nm, which matches the value determined from the TEM image mentioned above[6]. The XRD pattern also shows two broader peaks at 13° and 42° , corresponding to a shift of the

peaks associated with unfluorinated graphene to the left, indicating the emergence of new phases after fluorination. These can be attributed to the diffraction from the (001) and (100) lattice planes of fluorinated carbon materials. According to the Scherrer equation, the interlayer spacing d_{001} for all fluorinated graphite samples is calculated to be approximately 0.67 nm[7]. Therefore, when comparing the properties of the FG-0.95 sample and the Daikin sample, the influence of interlayer spacing on their performance is eliminated.

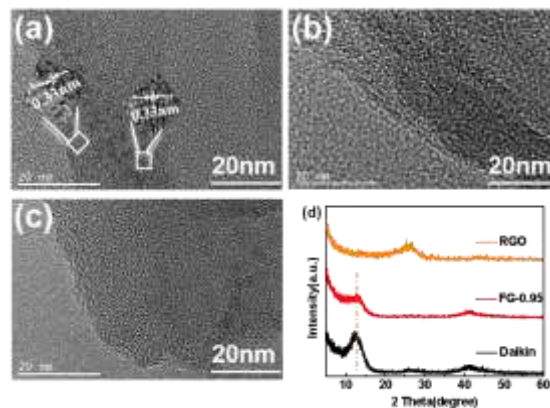


Fig.2 TEM images and XRD of materials.

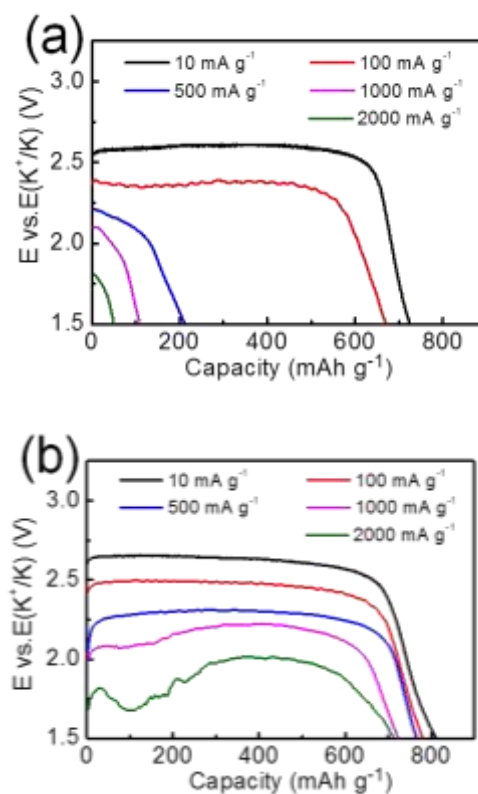


Fig.3 Discharge curves of (a) Daikin and (b) FG-0.95.

Fig.3 presents the galvanostatic discharge curves of FG-0.95 and Daikin samples as cathode materials for potassium-fluorinated carbon primary batteries at different current densities, with a cut-off voltage of 1.5 V. From Fig.3a, we can observe that when the current density is 10 mA g^{-1} , the discharge voltage of the Daikin sample is relatively stable, with a flat plateau region, and the initial discharge voltage is

approximately 2.6 V. Additionally, its specific capacity is relatively high, at about 720.1 mAh g⁻¹. When the current density increases to 2000 mA g⁻¹, it exhibits a similar trend to that at 1000 mA g⁻¹, with no stable discharge plateau, but the initial voltage has decreased to 1.8 V and the specific capacity has dropped to 50.6 mAh g⁻¹. Fig.3b displays the discharge curve of the potassium-fluorinated carbon primary battery with the FG-0.95 sample as the cathode material. From Figure b, we can see that when the current density is 10 mA g⁻¹, there is a relatively stable discharge plateau region with an initial discharge voltage of 2.6 V, which is similar to that of the Daikin sample, but its specific capacity is larger, at about 810.4 mAh g⁻¹. At a current density of 2000 mA g⁻¹, the plateau region experiences slight fluctuations due to the excessive current density, short discharge time, rapid diffusion, and imbalance of the discharge plateau. The initial discharge voltage is 1.8 V, which is similar to that of the Daikin sample, but its specific capacity remains high, at about 700.2 mAh g⁻¹. It is evident from both figures that at current densities of 500 mA g⁻¹, 1000 mA g⁻¹, and 2000 mA g⁻¹, the specific capacity of the FG-0.95 sample is much larger than that of the Daikin sample, indicating that FG-0.95 has better rate performance.

Based on the above analysis and comparison, it is evident that the overall discharge trend of the Daikin sample undergoes significant changes as the current density increases, while the overall discharge trend of the FG-0.95 sample remains relatively stable. The discharge voltage plateau of FG-0.95 is more stable, its specific capacity is larger, and its rate performance is better. Combining this with the analysis of the sample morphology from previous SEM characterization, it can be inferred that this is due to the smaller particle size of FG-0.95, which shortens the ion diffusion path and allows ions to better contact the carbon layer.

4. CONCLUSION

In this study, both Daikin and FG-0.95 samples were used as cathode materials for primary batteries to investigate the electrochemical performance of potassium-fluorinated carbon. Overall, the FG-0.95 sample demonstrates better electrochemical performance due to its favorable microstructure for ion diffusion, making it a promising candidate for cathode material in potassium-fluorinated carbon primary batteries. The excellent electrochemical performance of potassium fluorinated graphene primary batteries offers broad application prospects in various fields and has the potential to replace lithium batteries, significantly promoting the development of related industries to a certain extent

5. ACKNOWLEDGMENTS

The author sincerely thanks the School of Automotive Engineering of Zibo Vocational Institute for its strong support for this research.

6. REFERENCES

- [1] Zhou, H.P., et al., Plasma-enhanced fluorination of layered carbon precursors for high-performance CF_x cathode materials. *Journal of Alloys and Compounds*, 2023. 941.
- [2] Luo, Z., et al., Ultrafast Nano-Silver Modified Fluorinated Carbon Nanotubes Cathode Enables Advanced Lithium/Sodium/Potassium Primary Batteries. 2023.
- [3] Luo, Z., et al., Surface Engineering of Fluorinated Graphene Nanosheets Enables Ultrafast

Lithium/Sodium/Potassium Primary Batteries. *Adv Mater*, 2023. 35(40): p. e2303444.

- [4] Luo, Z., et al., Ultrafast Nano-Silver Modified Fluorinated Carbon Nanotubes Cathode Enables Advanced Lithium/Sodium/Potassium Primary Batteries. 2023.
- [5] Yue, H., et al., Reversible potassium storage in ultrafine CF : A superior cathode material for potassium batteries and its mechanism. *Journal of Energy Chemistry*, 2021. 53: p. 347-353.
- [6] Jiang, J., et al., The influence of electrolyte concentration and solvent on operational voltage of Li/CF primary batteries elucidated by Nernst Equation. *Journal of Power Sources*, 2022. 527.
- [7] Matsuo, Y., et al., Charge-discharge behavior of fluorine-intercalated graphite for the positive electrode of fluoride ion shuttle battery. *Electrochemistry Communications*, 2020. 110: p. 106626.